AIP Advances

Modulation of hole-injection in GaInN-light emitting triodes and its effect on carrier recombination behavior

Cite as: AIP Advances **5**, 107104 (2015); https://doi.org/10.1063/1.4932632
Submitted: 01 July 2015 . Accepted: 28 September 2015 . Published Online: 05 October 2015

Sunyong Hwang, Dong Yeong Kim, Jun Hyuk Park, Han-Youl Ryu, and Jong Kyu Kim

Modulation of hole-injection in GaInN-light emitting triodes and its effect on carrier recombination behavior

Sunyong Hwang,[1] Dong Yeong Kim,[1] Jun Hyuk Park,[1] Han-Youl Ryu,[2] and Jong Kyu Kim[1,a]
[1]*Department of Materials Science and Engineering, Pohang University of Science and Technology (POSTECH), Pohang, 790-784, Korea*
[2]*Department of Physics, Inha University, Incheon 402-751, Korea*

(Received 1 July 2015; accepted 28 September 2015; published online 5 October 2015)

The effects of the hole injection modulated by using a three-terminal GaInN-based light emitter, light-emitting triode (LET), on carrier recombination behavior and efficiency droop are investigated. It was found that the lateral electric field created by applying voltage bias between the two anodes effectively reduces efficiency droop as well as dynamic conductance of LETs. Detailed analyses of LETs under various operation conditions by APSYS simulations reveal that the asymmetry in carrier transport between electrons and holes is alleviated by promoted injection of hot holes over the potential barrier, increasing the hole concentration as well as the radiative recombination rate in the multiple quantum well active region. [http://dx.doi.org/10.1063/1.4932632]

The external quantum efficiency (EQE) of III-Nitride-based light emitting diodes (LEDs) has remarkably improved over the last two decades, enabling new energy-saving white light sources for mankind. However, GaInN LEDs suffer from a long-lasting EQE-loss mechanism called efficiency droop, a gradual decrease in LED efficiency with increasing driving current, which hinders a worldwide adsorption of LED-based solid-state lighting.[1–4] Although numbers of suspected droop-causing mechanisms such as Auger recombination,[5,6] delocalization of carriers,[7] and carrier leakage[8,9] have been suggested, the technical community does not have yet consent to a major single cause of efficiency droop.[10]

The asymmetry of carrier transport due to lower concentration and mobility of holes than those of electrons, which causes leakage of electrons out of the active region at high driving currents, was suggested as one of the major causes of efficiency droop.[11,12] Enhancement of the hole concentration at cryogenic temperatures by the field-enhanced ionization of acceptors[13,14] and improvement of hole-injection efficiency by energy-band-engineered electron-blocking layers (EBLs)[15,16] have been demonstrated to reduce efficiency droop, indicating that alleviation of such asymmetry is crucial for overcoming efficiency droop. Consequently, understanding the effect of the hole injection into the active region on radiative recombination behavior can provide an important clue for tackling efficiency droop by implementing suitable countermeasures. With light-emitting triodes (LETs) having two anodes, it was reported that injection of holes can be modulated by applying voltage biases between the two anodes, and enhanced hole-injection enabled by the LET mitigates efficiency droop.[17] However, the presence of the lateral electric field in the p-GaN layer of LETs under operation, and its effects on the recombination behaviors of injected carriers in the active region as well as on the electrical property of the device have not been systematically investigated with appropriate modeling and simulations based on experimental results.

In this study, we present the effect of the hole-injection modulated by the lateral electric field in the p-GaN layer of LETs on the transport of carriers and their recombination behaviors by using APSYS simulations. Variation of electrostatic potential distribution in LETs under various operating

[a]Electronic mail: kimjk@postech.ac.kr

conditions, and resultant distribution of injected holes and radiative recombination rate are investigated in detail. In addition, variation of dynamic conductance in LETs with varying anode-to-anode bias is measured and interpreted in terms of the hole temperature.

A commercial LED wafer with epitaxial structure consisting of a Si-doped n-GaN (electron concentration $n = 5 \times 10^{18}$ cm^{-3}), a 5-period of GaInN/GaN multiple quantum well (MQW) active region with peak emission wavelength of 440 nm, an AlGaN EBL, and a Mg-doped p-GaN was grown on c-plane sapphire substrate. Conventional LED fabrication process was employed for LET fabrication including mesa-etching by inductively-coupled plasma reactive ion etching, metallization of Ti/Al/Ni/Au (30/120/40/200 nm) ohmic contact for n-GaN, Ni/Au (20/200 nm) ohmic contact for p-GaN, followed by the deposition of Ti/Au (20/200 nm) pad metal. Fig. 1(a) shows top-view optical microscopy image of a LET (300×300 μm^2) with interdigitated two anodes, Anode 1 and Anode 2, on p-GaN. The spacing between the anodes is 8μm, so that a large modulation of lateral electric field inside the p-GaN layer is available by modulating anode-to-anode bias. Fig. 1(b) shows a schematic cross-sectional structure of the LET along the red line marked in Fig. 1(a), together with an equivalent circuit in the device. The lateral electric field along the p-GaN layer can be modulated by applying an anode-to-anode bias V_{A1A2}, which is the voltage difference between Anode1 (V_{A1C}) and Anode 2 (V_{A2C}) with respect to the cathode, so that the acceleration of holes by the field along the lateral direction of the p-GaN can be controlled. The higher the V_{A1A2}, the more the holes get accelerated. For the characterization of LETs, V_{A1A2} remains constant at each measurement sweep. For instance, in case of V_{A1A2} = 5 V, V_{A1C} is swept from 0 V to 7 V, while V_{A12} is swept from -5 V to 2V simultaneously. To examine the device with different hole-injection, V_{A1A2} is varied from 0 V to 10 V with 1 V step.

Relative EQE of the LET is estimated by light-output power divided by cathode current density considering the effective area modulation (EAM) model.[17] Fig. 2 depicts relative EQE as a function of current density of the LET at various V_{A1A2}. For all V_{A1A2}, conventional efficiency droop behavior is found, i.e., the LET shows a peak EQE at current densities ~ 10 A/cm^2, above which EQE gradually decreases. However, it is found that efficiency droop, defined in this study as (Peak EQE – EQE at 100 A/cm^2) / Peak EQE, significantly decreases from ~25 % to ~10 % by increasing the V_{A1A2}, as shown in the inset of Fig. 2. It remarks that droop-causing component is alleviated by increasing V_{A1A2}, consistent with the previous report.[17]

The distribution of holes and radiative recombination rates in the LET structure, and resultant IQE at various V_{A1A2} conditions are calculated by using APSYS device simulator. A simplified vertical LET structure having two anodes on p-GaN with 8 μm spacing between them, and cathode on n-GaN, as shown in the inset of Fig. 3, is used for the simulation. Typical parameters for GaInN-based LEDs epitaxial structure grown on a c-plane sapphire substrate are used, including SRH lifetime of 3 ns, and spontaneous and piezoelectric polarization charge densities of 7.01×10^{12} cm^{-2} and 3.92×10^{12} cm^{-2} in the MQW and EBL, respectively.[18] For the realization of LET operation conditions, same sets of

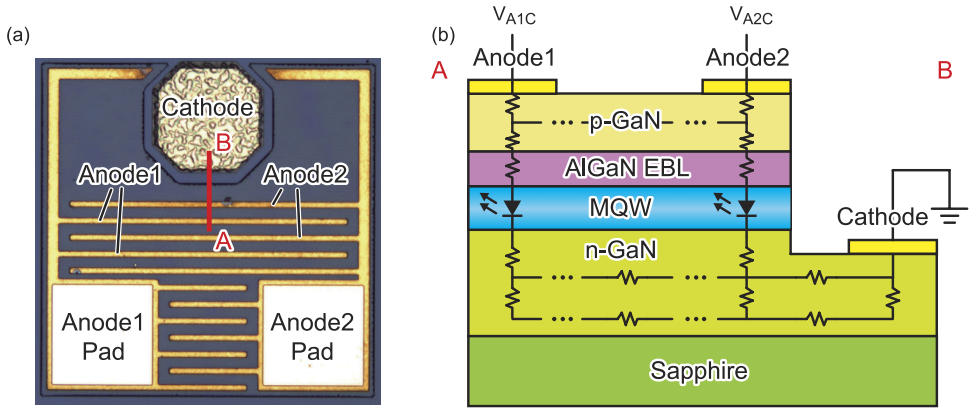

FIG. 1. (a) Top-view optical microscopy image of the fabricated LET device having two anodes, Anode 1 and Anode 2, and a cathode. (b) Schematic cross-sectional view of the red line in Fig. 1(a) of the LET device with an electrical circuit design.

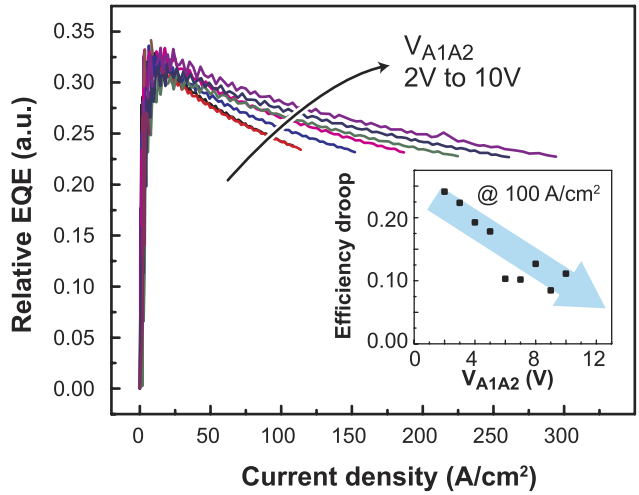

FIG. 2. Relative external quantum efficiency (EQE) as a function injection current density at different anode-to-anode biases (2 V ~ 10 V) measured at room temperature. Inset shows efficiency droop at 100 A/cm^2 as a function of anode-to-anode bias.

V_{A1C} and V_{A2C} with those for used for experimental measurements are implemented. Fig. 3 shows calculated IQE at various V_{A1A2} ramping from 1V to 10V as a function of cathode current density. Efficiency droop is reduced with increasing V_{A1A2}, consistent with experimental results shown in Fig. 2.

Distribution of holes during the device operation at a steady state gives important information on the carrier transport and recombination processes in the device. Figs. 4(a) and 4(b) show the distribution of hole concentration in each layer across the whole device and radiative recombination rate at the last quantum well (QW), respectively, calculated at V_{A1C} = 3.5 V with V_{A1A2} ramping from 0 to 10 V by using APSYS simulator. Hole concentration at the last QW increases as V_{A1A2} increases, as shown in the magnified curves of red squared region in the inset of Fig 4(a), indicating enhancement of hole injection from the p-GaN over the EBL into the active region by applying V_{A1A2}. Accordingly, radiative recombination rate in the QW increases as shown in Fig. 4(b). Inset of Fig. 4(b) shows the peak intensity of radiative recombination rate at the last QW as a function of V_{A1A2}, clearly showing enhancement of light output with increasing V_{A1A2}, which is attributed to increased hole-injection into the active region enabled by electric field between two anodes.

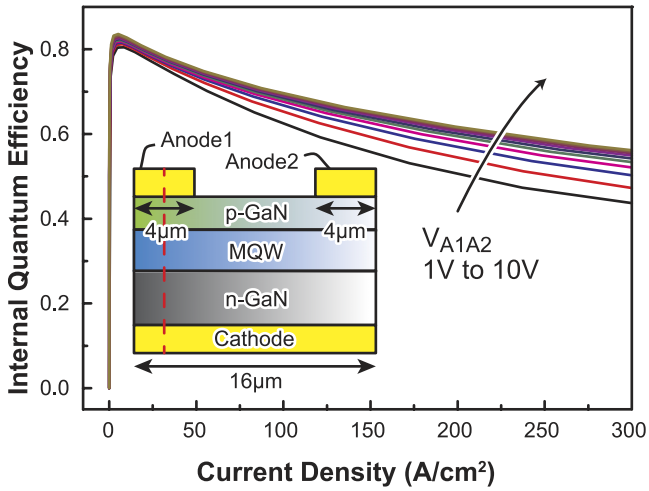

FIG. 3. Internal quantum efficiency (IQE) of an LET shown in inset as a function of current density at various V_{A1A2} from 1 V to 10 V simulated by APSYS device simulator. The inset describes simulated structure with two anodes with spacing of 8 μm between them, and one cathode.

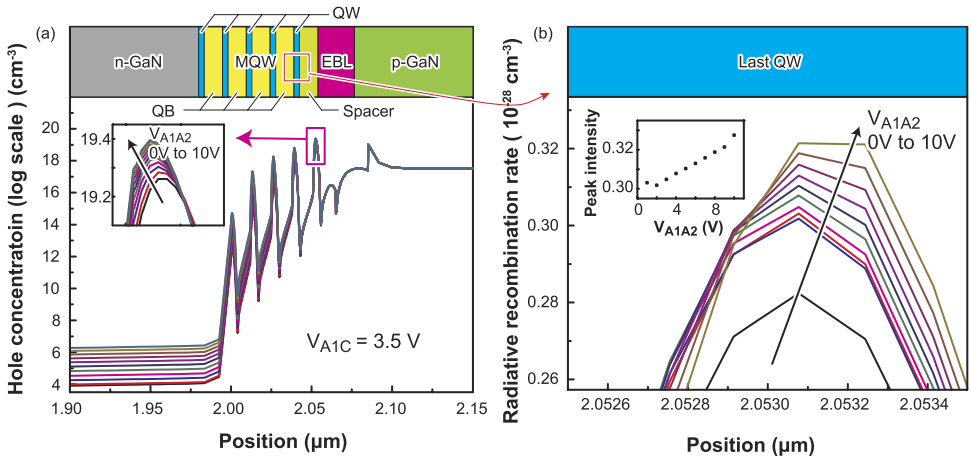

FIG. 4. (a) Distribution of hole concentration in each layer constituting the whole LET under V_{A1C} = 3.5 V and varied V_{A1A2} from 0 V to 10 V. The inset shows a magnified view of the hole concentration of the last quantum well (QW) close to p-GaN. (b) Radiative recombination rate in last QW. The inset shows the peak intensity of radiative recombination rate at the last QW as a function of V_{A1A2}.

The effect of V_{A1A2} on the electrostatic potential, thus electric field distribution over the whole LET structure is investigated. Fig. 5(a) shows three-dimensional contour map of the electrostatic potential over the whole LET structure under operating condition of V_{A1A2} = 5 V and V_{A1C} = 3.5 V calculated by APSYS simulation. A deep potential "valley" is formed in the p-GaN layer near Anode 2 due to negative voltage bias applied to Anode2. Electrostatic potential in the horizontal direction along the p-GaN layer linearly drops from Anode 1 to Anode 2, while that in the n-GaN layer shows almost no change, indicating that the V_{A1A2} creates an electric field along the p-GaN which can accelerate the holes in the horizontal direction. Fig. 5(b) depicts the electrostatic potential between the two anodes with varying V_{A1A2}. For all cases, the electrostatic potential linearly decreases from Anode 1 to Anode 2. As V_{A1A2} increases, the difference in the electrostatic potential between the two anodes increases as well, resulting in higher electric field in the lateral direction along the p-GaN, as shown in inset of Fig. 5(b). Note that increased electric field by applying a high V_{A1A2} is likely to produce hot holes with energy enough to overcome the potential barrier between the p-GaN and EBL, thus increase the injection efficiency of holes into the active region.

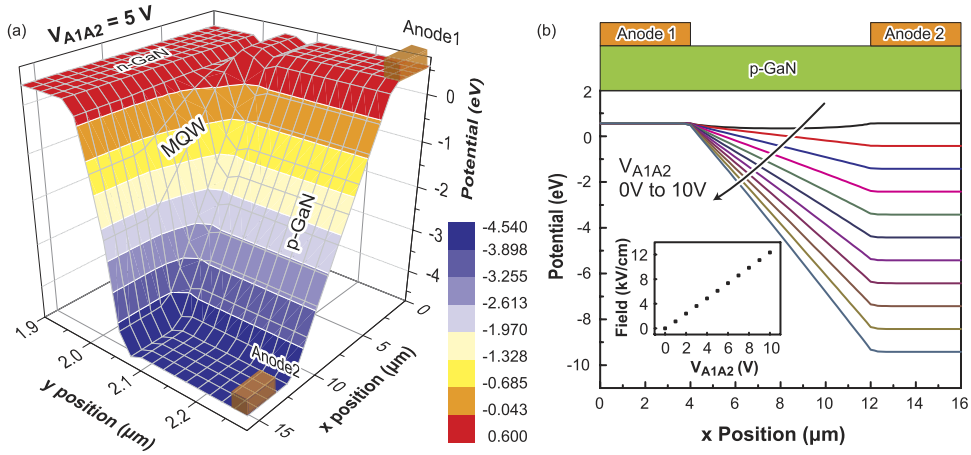

FIG. 5. (a) Three-dimensional contour map of the electrostatic potential energy in LET over p-GaN, MQW, and n-GaN region under V_{A1A2} = 5 V and V_{A1C} = 3.5 V. (b) Electrostatic potential distribution along horizontal direction of the p-GaN between the two anodes under various V_{A1A2}. The inset shows the electric field along the horizontal direction in the p-GaN between Anode 1 and Anode 2.

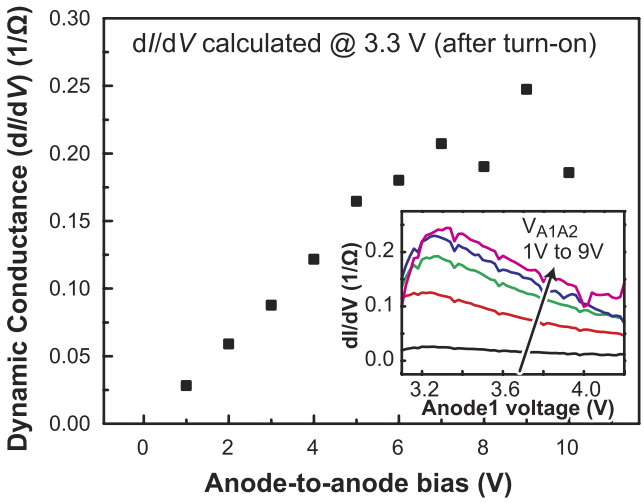

FIG. 6. Dynamic conductance calculated at the V_{A1C} of 3.3 V as a function of anode-to-anode bias. The inset shows the dynamic conductance as a function of Anode 1 voltage at various V_{A1A2}.

In order to investigate the effect of V_{A1A2} modulation on the electrical property of the LET, dynamic conductance (dI/dV) is calculated from current-voltage (I-V) characteristic of the LET at various operating conditions. Current collected from Anode 1 is used for calculating the dynamic conductance due to the difficulty in independent analysis of cathode current dependency on V_{A1C}. Fig. 6 shows the dynamic conductance measured at 3.3 V (after turn-on) as a function of V_{A1A2}. The inset shows Anode 1 voltage dependent dynamic conductance at various V_{A1A2}. Dynamic conductance increases linearly with V_{A1A2}, which is mainly attributed to increase in electrical conductivity in the p-GaN layer.

Under an LET operating condition, holes are accelerated gaining energy by the lateral electric field in the p-GaN between two anodes, resulting in redistribution of holes with respect to energy in the valence band.[19] As hot electrons in metal oxide semiconductor field-effect transistors are responsible for the gate leakage through gate oxide,[20] accelerated hot holes by V_{A1A2} likely to have enough energy to overcome the potential barrier, flying over the EBL into the active region. Valence band offset between p-GaN and AlGaN EBL is regarded as unintentional energy barrier for injection of holes, prohibiting their injection into active region, thus aggravating the asymmetry in transport between electrons and holes, which consequently causes the flow of electrons through the active region without recombining, i.e., electron leakage. Let us consider an LET under operation condition of $V_{A1A2} = 0$ V and $V_{A1C} = 3.5$ V. The energy difference between hole quasi-Fermi level of p-GaN and valence band edge of EBL under the operation condition is calculated to be 0.27 eV by APSYS simulation, which is the energy barrier for hole injection into the active region. Fraction of holes overcoming energy barrier can be estimated by utilizing Maxwell-Boltzmann distribution which describes the number of carriers with respect to energy at a temperature. Assuming the measurement temperature of 300 K and $V_{A1C} = 3.5$ V, fraction of holes overcoming the energy barrier is only ~0.3%. Next, let us consider the LET under lateral electric field E by applying V_{A1A2}. The hole temperature, T_h, is given by

$$T_h - T = e\mu_h E^2 \tau_e \frac{2}{3k},$$

where T is lattice temperature, μ_h is hole mobility in p-GaN region, and τ_e is optical phonon scattering time. $\mu_h = 10\ \mathrm{cm^2\ V^{-1}\ s^{-1}}$ and $\tau_e = 10^{-12}$ s are used for the calculation.[21] Under V_{A1A2} of 10 V, $T_h - T = 12$ K, the fraction of energetic holes overcoming the energy barrier between the p-GaN and the EBL is increased by 45% compared to that without lateral electric field, resulting in increase of dynamic conductance through the device, as well as increase in hole concentration into the active region in accordance with the simulation result shown in Fig. 4(a). Note that $T_h - T$ can be more increased either by applying higher V_{A1A2} or by using smaller distance between two anodes at the same V_{A1A2}, which promotes injection of holes into MQW region, thereby further reducing efficiency droop.

LET may not be a practical visible light emitter due to additional voltage bias required for operation and more complex circuit design. However, it can provide a deep understanding of physical mechanism responsible for limited efficiency and efficiency droop, thus a clue for suitable countermeasures to overcome the long-lasting problem in GaInN-based LEDs. In addition, the LET can be a practical, we believe, deep ultraviolet light emitter because the EQE of conventional AlGaN-based deep ultraviolet LEDs is fundamentally limited by extremely severe asymmetry in carrier transport which can be effectively alleviated by LETs.[14]

In summary, the effect of the hole-injection modulated by the lateral electric field in the p-GaN layer on both optical and electrical properties of a three-terminal light emitter, LET, is systematically investigated. It is found that efficiency droop is reduced from ~25 % to ~10 % at 100 A/cm^2 by increasing V_{A1A2} from 2 V to 10 V. APSYS simulations on the LET under various operation conditions show that both hole concentration and radiative recombination rate at the active region increase with increasing V_{A1A2}, thus, reduced efficiency droop. These consistent results can be explained in terms of the alleviated asymmetry in carrier transport enabled by promoted hole injection into the active region. Variations in electrostatic potential in the horizontal direction along the p-GaN layer linearly drops from Anode 1 to Anode 2, indicating that the V_{A1A2} creates an electric filed along the p-GaN which can accelerate the holes in the horizontal direction. Applying lateral electric field in the p-GaN accelerates holes increasing the hole temperature, therefore the number of holes that can overcome the potential barrier at the GaN spacer and the EBL increases, promoting the injection of holes into the active region, which is supported by increased dynamic conductance calculated from the current-voltage characteristics.

The Authors gratefully acknowledge supports by the International Collaborative R&D Program of Korea Institute for Advancement of Technology (KIAT) (M0000078, Development of Deep UV LED Technology for Industry and Medical Application), and the Brain Korea 21 PLUS project for Center for Creative Industrial Materials (F14SN02D1707).

[1] S. Nakamura, Science **281**, 956 (1998).
[2] J. Jaehee, E. F. Schubert, and J. K. Kim, Laser Photonics Rev. **7**, 408 (2013).
[3] T. Fujii, Y. Gao, R. Sharma, E. L. Hu, S. P. DenBaars, and S. Nakamura, Appl. Phys. Lett. **84**, 855 (2004).
[4] M. H. Kim, M. F. Schubert, Q. Dai, J. K. Kim, E. F. Schubert, J. Piprek, and Y. Park, Appl. Phys. Lett. **91**, 183507 (2007).
[5] J. Iveland, L. Martinelli, J. Peretti, J. S. Speck, and C. Weisbuch, Phys. Rev. Lett. **110**, 177406 (2013).
[6] M. Zhang, P. Bhattacharya, J. Singh, and J. Hinckley, Appl. Phys. Lett. **95**, 201108 (2009).
[7] B. Monemar and B. E. Sernelius, Appl. Phys. Lett. **91**, 181103 (2007).
[8] G. Lin, D. Meyaard, J. Cho, E. F. Schubert, H. Shim, and C. Sone, Appl. Phys. Lett. **100**, 161106 (2012).
[9] D. S. Meyaard, G. Lin, Q. Shan, J. Cho, E. F. Schubert, H. Shim, M. H. Kim, and C. Sone, Appl. Phys. Lett. **99**, 251115 (2011).
[10] J. Piprek, F. Romer, and B. Witzigmann, Appl. Phys. Lett. **106**, 101101 (2015).
[11] J. Xu, M. F. Schubert, A. N. Noemaun, D. Zhu, J. K. Kim, E. F. Schubert, M. H. Kim, H. J. Chung, S. Yoon, C. Sone, and Y. Park, Appl. Phys. Lett. **94**, 011113 (2009).
[12] J. Xie, X. Ni, Q. Fan, R. Shimada, U. Ozgur, and H. Morkoc, Appl. Phys. Lett. **93**, 121107 (2008).
[13] G. Lin, Q. Shan, Y. Wang, T. Li, and E. F. Schubert, Appl. Phys. Lett. **105**, 221116 (2014).
[14] J. H. Park, G. Lin, D. Y. Kim, J. W. Lee, J. Cho, J. Kim, J. Lee, Y. Kim, Y. Park, E. F. Schubert, and J. K. Kim, Opt. Exp. **23**, 15398 (2015).
[15] C. H. Wang, C. C. Ke, C. Y. Lee, S. P. Chang, W. T. Chang, J. C. Li, Z. Y. Li, H. C. Yang, H. C. Kuo, T. C. Lu, and S. C. Wang, Appl. Phys. Lett. **97**, 261103 (2010).
[16] J. H. Park, D. Y. Kim, S. Hwang, D. Meyaard, E. F. Schubert, Y. D. Han, J. W. Choi, J. Cho, and J. K. Kim, Appl. Phys. Lett. **103**, 061104 (2013).
[17] S. Hwang, W. J. Ha, J. K. Kim, J. Xu, J. Cho, and E. F. Schubert, Appl. Phys. Lett. **99**, 181115 (2011).
[18] F. Bernardini, in *Nitride Semiconductor Devices: Principles and Simulation*, edited by J. Piprek (Wiley-VCH, Weinheim, 2007), pp. 49–67.
[19] W. E. Pinson and R. Bray, Phys. Rev. **136**, A1449 (1964).
[20] C. Duvvury, D. J. Redwine, and H. J. Stiegler, IEEE Elec. Dev. Lett. **9**, 579 (1988).
[21] J. K. Kim, E. F. Schubert, J. Cho, C. Sone, J. Y. Lin, H. X. Jiang, and J. M. Zavadad, J. Electrochem. Soc. **153**, G734 (2006).